LARGE TRANSIENT NONPROTON ION MOVEMENTS IN PURPLE MEMBRANE SUSPENSIONS ARE ABOLISHED BY SOLUBILIZATION IN TRITON X-100

TIM MARINETTI AND DAVID MAUZERALL
The Rockefeller University, 1230 York Avenue, New York, New York 10021

ABSTRACT Light-induced release/uptake of both protons and other ions cause transient changes in conductivity in suspensions of purple membrane (PM) fragments (Marinetti, Tim, and David Mauzerall, 1983, *Proc. Natl. Acad. Sci. USA*, 80:178–180). We find that the release/uptake of nonproton ions with quantum yield >1 is observed at most pHs and ionic strengths. Only at both low pH and low ionic strength is the conductivity transient mostly due to protons. Our hypothesis is that during the photocycle, changes occur in the PM's dense surface charge distribution that result in changes in the number of counterions bound or condensed at the membrane surface. To test this, the PM structure was perturbed with the nonionic detergent Triton X-100. Immediately after addition, Triton does not abolish the nonproton ion movements; in fact at low detergent concentrations (0.02% vol/vol) the signal amplitudes increased considerably. However, when PM is completely solubilized into monomers in Triton, the conductivity transients are due to protons alone, though at lower quantum yield compared with native PM. These results suggest that changes in the surface charge distribution in native PM's photocycle could contribute to proton transfer between the aqueous phase and bR itself.

INTRODUCTION

The purple membrane of *Halobacterium halobium* is a highly ordered two-dimensional lattice containing a single protein, bacteriorhodopsin (bR), which makes up about 75% of the mass, the rest being lipid. Bacteriorhodopsin is known to be a light-driven proton pump, as first proposed by Oesterhelt and Stoeckenius (1973). Proton pumping occurs when bR is present in monomeric form, as shown in experiments with it incorporated into phospholipid vesicles (Dencher and Heyn, 1979). For reviews of the extensive literature that has accumulated about this fascinating system see Henderson (1977), Stoeckenius et al. (1979), Stoeckenius and Bogomolni (1982), and Dencher (1983).

Light-induced proton translocation by bR is a fact well established by measurements on PM fragments, whole cells, cell envelope vesicles, and in both artificial phospholipid vesicles and planar bilayers. The methods employed have included pH indicator dyes (e.g. Lozier et al., 1976; Govindjee et al., 1980; Dencher and Wilms, 1975; Drachev et al., 1984), volume changes (Ort and Parson, 1978), and steady state measurements of light-induced pH changes (e.g., Renthal, 1981; Dencher and Heyn, 1979; Happe et al., 1977; Ramirez et al., 1983). We cite only representative examples—the literature contains numerous other reports.

The PM is expected to have a substantial negative surface charge both because of the charged amino acid side chains of bR and from the lipids of the PM, some of which are negatively charged (Kushwaha et al., 1976). This is suggested in the various models for the folding of the polypeptide chain, both those consisting solely of transmembrane helices (Ovchinnikov et al., 1979; Engelman et al., 1980; Agard and Stroud, 1982) and one that involves helices and beta sheet (Jap et al., 1983). Experimental evidence for a net negative surface charge comes from electron microscopy studies that showed binding of PM to polylysine-treated glass (Fisher et al., 1978) and ferritin binding to the PM (Neugebauer et al., 1978). Orientation of the PM in weak electric fields (Kimura et al., 1981; Keszthelyi, 1980; Druckmann and Ottolenghi, 1981) indicates it has a large permanent dipole moment. Attempts to measure both the static surface potential and light-induced changes in it have been performed using Electron Paramagnetic Resonance (EPR) (Tokutomi et al., 1980; Carmeli et al., 1980), resonance Raman (Ehrenberg and Meiri, 1983; Ehrenberg and Berezin, 1984) and optical absorbance (Carmeli and Gutman, 1982) techniques using charged probe molecules as well as measurement of the PM's electrophoretic mobility (Packer et al., 1984).

Most of the above measurements were interpreted in terms of charge changes at the PM surface associated with the release of protons during the photocycle since this would be expected to lead to an increase in the negative charge of the PM. Slifkin et al. (1978, 1979) reported conductivity changes in PM suspensions and suggested that ions other than protons could be involved; this was subsequently proven (Marinetti and Mauzerall, 1983).

Here we show that at high ionic strength, nonproton ion escape and recapture with a quantum yield far in excess of 1 are always observed. These are abolished by complete solubilization of the PM in the nonionic detergent Triton X-100: the remaining conductivity changes are then small and primarily due to protons. We suggest that the native PM undergoes light-induced changes in the counterions condensed on its surface and that the surface potential changes responsible for this may contribute significantly to proton pumping. A preliminary report of these results was presented at a Biophysical Society meeting (Marinetti and Mauzerall, 1985).

MATERIALS AND METHODS

The differential ac conductivity bridge was described previously (Marinetti and Mauzerall, 1983). (There is a typographical error therein: the cell capacitance is 1.0 μF not 0.1 μF.) An Osborne 1 microcomputer was used to perform nonlinear least-squares fits to obtain the amplitudes and time constants of the conductance transients. Earlier experiments on PM suspensions were performed at ambient temperature (25°–28°C); susbsequent work including that using bR monomers was done at 16°C in a home-built temperature-controlled block. Temperature control is provided by a circulating bath (model 5003; Hart Scientific), rated at ± 0.0005°C. The high thermal mass of the block (~40 kg of brass and 25 liters of coolant) gives the extremely high thermal stability required to perform the conductivity experiments either at temperatures other than ambient, or when using long time base sweeps. We measure a drift of variable sign between the two cells of the bridge of <0.00015°C/s. This drift is linear and it can be easily corrected by baseline subtraction.

Our method employs a high frequency ac bridge with a lock-in amplifier to detect "off balance" signals between two identical conductivity cells. The high frequency eliminates electrode polarization effects and gives millisecond time resolution. Slifkin et al. (1978, 1979) detected conductivity changes using a modulation technique employing chopped light. They also used the heating of the solution by absorbed light to set the absolute detector phase since a temperature increase necessarily increases the conductivity of all ions. We have employed the thermal heating effect both for this purpose and to obtain absolute quantum yields.

pH measurements were done using a Radiometer model 4 pH meter with an Ingold 6023-03 combination electrode. All chemicals were reagent grade; imidazole (Sigma Chemical Co., St. Louis, MO) was twice recrystallized from benzene following treatment with activated charcoal.

Halobacterium halobium strain S-9 were grown from a slant kindly provided by Dr. W. Stoeckenius and purple membranes were prepared as described in Oesterhelt and Stoeckenius (1974). PM was stored in 3 M NaCl at 4°C. Solubilization of bR into monomers in Triton X-100 was performed following the procedure of Dencher and Heyn (1982). By solubilized, we refer to material that does not sediment after a 90-min spin at 38,000 rpm (Beckman Ti-50 rotor, L2-65 ultracentrifuge) after at least 20 h incubation in the detergent (0.3–0.4% vol/vol) at room temperature in the dark at pH 7 and low ionic strength. The transient conductance experiments were performed on samples with an optical density of between 0.5 and 0.7 at 570 nm. This is ~10 μM bR.

Conductance titrations to determine *pK* and equivalent conductance information for buffers were done at room temperature using a conductance meter (model 35; Yellow Springs Instrument Co., Yellow Springs, OH) with a YSI probe (model 3403; Yellow Springs Instrument Co.). Calibrations were done with known concentrations of KCl. Concentration and temperature dependences of the equivalent conductances of common ions were interpolated from published tables (Dean, 1979; Washburn, 1929).

The analysis of the conductivity transients is based on Eq. 1 of Marinetti and Mauzerall (1983)

$$\phi\Lambda = \left(\frac{S_P}{S_T}\right) \cdot \frac{N_0 \epsilon}{1{,}000\, C\rho} \cdot \sum_i c_i \Lambda_i \left(\frac{1}{\Lambda_i}\frac{d\Lambda_i}{dT}\right), \qquad (1)$$

where ϕ is the quantum yield of the ion transiently released or uptaken during the photocycle, Λ is its effective equivalent conductance, S_P and S_T are the transient and thermal signal amplitudes (see Results). N_0 is Avogadro's number, ϵ is the energy of the photon (3.4×10^{-19} J at 584 nm), C is the heat capacity of the solution, and ρ is its density. The sum extends over all ions in the solution where c_i is the concentration, Λ_i is the equivalent conductance and the term in parentheses is the temperature coefficient of the conductance. The latter is 0.022/°C for all ions except H^+ and OH^-. If more than one ion is transiently moved after the light flash, $\phi\Lambda$ is the sum of the products for each ion.

The effective equivalent conductance above is the change per equivalent upon introduction of the ion into the solution. For a simple ion like sodium, this is identical to the equivalent conductance. For protons, it is the weighted average of the conductance changes caused by an incremental addition of strong acid to the buffer system employed. This can be calculated from the conductances of the protonated and deprotonated forms of the buffer and its *pK*. (See Appendix). The product of the heat capacity and density varies slightly from 1.0 in water to 0.967 in 1 M NaCl.

EXPERIMENTAL RESULTS

The experiments presented below measure the transient light-induced conductance changes in PM suspensions in 1.1 M NaCl in the pH range 4–8. We have also examined the effect of the nonionic detergent Triton X-100 both immediately after addition to the PM suspensions and after complete solubilization into bR monomers. Before describing the results, we must point out several important features of our experimental methodology. First, the conductivity of a solution is directly proportional to $\Sigma_i c_i \Lambda_i$, where c_i is the concentration of ion i and Λ_i is its equivalent conductance. The actinic light flash can cause both the concentrations of some ions to change, via the photochemical reaction cycle, and also the equivalent conductance of all ions to increase due to the heating of the solution by the degradation of the absorbed photons. This appears as a constant baseline shift since thermal relaxation of the sample + cell is very slow (~2 min) compared with the bR photocycle. If the exciting light is in the linear range of photoresponse, the ratio of the transient signal to the thermally shifted baseline is directly proportional to the absolute quantum yield—the method is internally calibrated (Marinetti and Mauzerall, 1983).

Second, we detect only small mobile ions. Changes in conductance due to changes in the charges on the PM itself are negligible because: (*a*) the fragments are very large and hence have low mobility; and (*b*) even though the fragments are highly charged, much if not most of this charge is screened by condensed counterions.

Third, transients due to proton release and/or uptake can be distinguished from those due to other ions by changing the composition of the buffer. For example, transient uptake of protons by the PM fragments is equivalent to an addition of a strong base. In an "acidic"

buffer such as acetic acid/acetate, this would result in the net creation of ions (neutral acetic acid goes to charged acetate ion). In a "basic" buffer such as ammonia/ammonium the same proton uptake would result in the net loss of ions (charged ammonium goes to neutral ammonia). Hence if we vary the composition of the buffer by trading off two opposite kinds of buffers with similar *pK* values we can cause the magnitude and sign of the conductance transient to change in a predictable manner if the signal is due to proton movements. (See the Appendix for the calculation.) Conversley, if the signal does not show the expected variation with buffer changes, it cannot be due to protons.

Earlier we showed (Marinetti and Mauzerall, 1983) that at low ionic strength at pH 4, the conductance changes could be well described by fast proton uptake by the PM after the flash. In acetate buffer this results in a positive signal that decays as the protons are released by the PM at the end of the photocycle. Fig. 1 shows the results at low pH in 1.1 M NaCl, an ionic strength closer to physiological conditions. Trace *A* is the PM "as is" with no external buffers except for dissolved carbon dioxide (which lowers the pH from 7 to about 5). The sharp spike in the first few milliseconds after the flash is an electrical artifact due to the laser discharge and can be seen in the absence of bR. The transient signal, in this case negative, has a rise time that is limited by the time constant of the lock-in amplifier (1 ms). It relaxes with a decay time ($1/e$) of 8.8 ms to a baseline shifted above that before the flash—this is the heating effect discussed above. Traces *B* and *C* show the effect of adjusting the pH with HCl and NaOH to 3.7 and 3.99, respectively. Note that the amplitude of the signal is sharply reduced. Traces *D* and *E* show the same sample after acetate buffer is added at 2 and 25 mM, respectively. The latter concentration is well in excess of the stray carbon dioxide and any of the buffering groups on the PM. Yet the signal amplitude is virtually unaffected. If the transient signal were due to protons, it should have changed sign but it does not. Finally, traces *F*, *G*, and *H* show the effect of increasing the pH stepwise a total of 1 unit. The signal amplitude clearly increases, but it remains negative and does not grow to the size observed in the absence of buffer. The time constant of the signal remains unchanged throughout. We conclude that at pH 4 in 1.1 M NaCl the ion movements we detect are in their majority not due to protons.

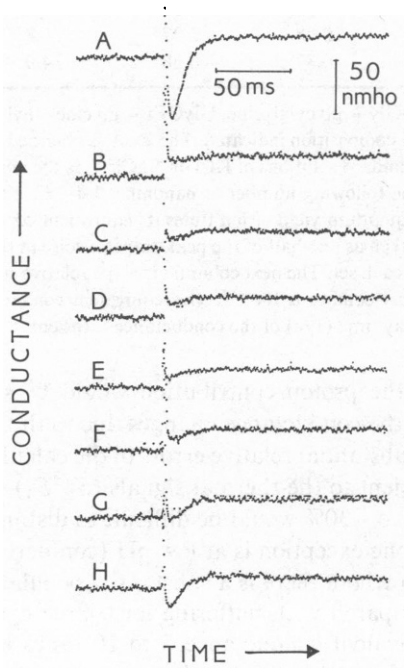

FIGURE 1 Light-induced conductance changes in purple membrane suspensions at low pH in 1.1 M NaCl. Buffer and pH for each trace are given in Table I, samples 1-*A*–1-*H*. Each trace is the sum of 64 flashes.

The quantitative results from this and analogous experiments at pH 5, 7, and 8 in 1.1 M NaCl are given in Table I. The basic conclusion is that protons cannot be responsible for the bulk of the conductivity changes detected. If one compares the columns giving the observed and expected relative amplitudes when the buffer composition is varied at constant pH, there is a marked discrepancy: the expected sign changes do not occur.

At pH 5 (Table I; samples 2 *A–E*), addition of acetate to trimethylamine oxide buffered PM fragments does not invert the signal sign. Instead of the expected zero-crossing at sample 2 *B*, we observe a slight increase in signal amplitude upon addition of acetate and no further changes thereafter. The low pH proton uptake by low ionic strength PM suspensions observed using absorbance changes in a pH indicating dye (Dencher and Wilms, 1975) should give a positive signal in acetate buffer whereas we observe uniformly negative signals. It is true that the ionic strength of the samples used here is much higher than used by Dencher and Wilms (1975); also, the question of the order of proton release and uptake is controversial. Mitchell and Rayfield (1986) claim that protons are first released then uptaken at low pH, in disagreement with our earlier report of proton uptake (Marinetti and Mauzerall, 1983). At this time we do not have any explanation for the difference. We note that Bogomolni et al. (1986) have confirmed our claim of proton uptake at low pH using a fast pH electrode.

At pH 7 and 8, the transients are positive in sign. This is expected for proton release into an imidazole buffer (Table I; sample 3 *A*) but not for glycylglycine (sample 4 *A*). Again, addition of the opposing buffer, in these cases phosphate and glycine ethyl ester respectively, does not cause the sign inversion expected if the transient was solely due to protons.

These data do not exclude proton movements; rather, the proton contribution to the observed transients is small compared to that of other ions. While we cannot specify what ions are responsible for the signal, we can conclude that the quantum yield for the process is greater than 1.

TABLE I
bR IN 1.1M NaCl

Sample	pH	Buffers*		$\Sigma c_i\Lambda_i$	S_P	S_T	S_P/S_T	$\phi\Lambda$	Relative error	Relative signal	Calculation for H^+ alone	Calculation of Λ per mole H^+	Decay time
									%				*ms*
		OAc											
1*A*	5.1	0		84.4	−7.6	1.9	−4.0	−376	14	(1)	(1)	304	8.8
1*B*	3.7	0		84.4	−0.3	1.9	−0.16	−15	81	0.04	1.14	349	—
1*C*	3.99	0		86.6	−0.7	1.7	−0.41	−40	39	0.10	1.14	348	9.5
1*D*	3.97	2.37		86.6	−0.65	1.9	−0.34	−33	39	0.09	0.21	64.4	8.4
1*E*	4.02	25.4		84.4	−0.75	1.7	−0.44	−41	36	0.10	−0.10	−30.2	8.9
1*F*	4.33	25.2		84.4	−0.90	1.9	−0.47	−44	30	0.11	−0.12	−37.4	9.4
1*G*	4.65	25.1		85.8	−1.9	1.75	−1.09	−104	20	0.27	−0.13	−39.6	8.0
1*H*	5.02	25.0		84.8	−3.1	1.35	−2.30	−217	20	0.58	−0.13	−40.4	8.1
		TMAO	OAc										
2*A*	5.09	4.74	0	80.9	−9.5	3.5	−2.7	−243	15	(1)	(1)	42.7	10.0
2*B*	5.08	4.71	4.71	80.9	−8.5	2.4	−3.5	−315	21	1.3	−0.05	−2.0	9.6
2*C*	5.01	4.69	9.37	82.3	−8.2	1.9	−4.3	−394	26	1.6	−0.35	−15.1	8.3
2*D*	5.03	4.63	23.2	84.4	−8.1	1.9	−4.3	−404	26	1.6	−0.67	−28.4	8.0
2*E*	5.08	4.53	36.2	84.4	−7.1	2.0	−3.6	−338	32	1.3	−0.77	−32.8	8.6
		Imid	Phos										
3*A*	7.22	4.74	0	91.8	7.5	4.3	1.74	178	7	(1)	(1)	35.8	16
3*B*	7.08	4.73	2.36	88.0	6.4	2.3	2.78	272	12	1.6	0.15	5.3	17
3*C*	7.12	4.71	4.71	89.5	5.5	2.3	1.47	146	12	0.84	−0.28	−10.0	19
3*D*	7.23	4.68	9.36	91.8	7.3	2.5	2.92	298	11	1.68	−0.71	−25.4	21
3*E*	7.15	4.63	18.5	91.8	5.1	1.9	2.68	274	14	1.54	−1.05	−37.6	23
3*F*	7.23	4.50	45.0	93.3	7.2	2.6	2.76	287	10	1.59	−1.33	−47.6	18
		GlyGly	GlyOEt										
4*A*	7.98	4.71	0	95.7	10.8	1.2	9.0	960	17	(1)	(1)	−24.3	83
4*B*	8.10	4.69	2.35	98.1	12.9	1.3	9.9	1082	16	1.1	0.35	−8.6	93
4*C*	8.08	4.67	4.67	95.1	11.6	1.4	8.3	879	14	0.92	0.01	−0.3	91
4*D*	8.14	4.64	9.28	99.7	11.5	1.3	8.8	977	15	0.98	−0.27	6.8	93
4*E*	8.10	4.57	18.3	99.7	12.4	1.6	7.8	866	13	0.87	−0.58	14.0	81

*OAc = acetate; TMAO = trimethylamine oxide; Imid = imidazole; Phos = phosphate; GlyGly = glycylglycine; GlyOEt = glycine ethyl ester.
Bacteriorhodopsin in 1.1 M NaCl, pH 4 to 8. The data for each pH are set off, with the buffer composition indicated. The $\Sigma_i c_i\Lambda_i$ is obtained from the bulk conductivity of the solution, calculated from the observed cell resistance compared against standard solutions of KCl or NaCl. S_p is the amplitude of the transient signal and S_T is the thermal signal in arbitrary units. One unit is equivalent to the following number of nanomho: 1*A*–1*H*, 20; 2*A*–2*E*, 9.6; 3*A*–3*F*, 21; and 4*A*–4*E*, 46. From the ratio S_p/S_T we calculate the $\phi\Lambda$, the product of the quantum yield of ion times its equivalent conductance (see Methods). The relative error in $\phi\Lambda$ is dominated by the errors in S_p and S_T, which we have taken as one-half of the peak-to-peak noise in the traces. The relative signal is the value of $\phi\Lambda$ normalized both in sign and magnitude to the first sample in each set. The next column gives the relative signal expected if the signal was due to H^+ alone, and with the quantum yield constant. The second to last column is the effective equivalent conductance change calculated for the buffer mixture in each sample (see Appendix). The final column is the decay time ($1/e$) of the conductance transient.

Since the equivalent conductance for a nonproton ion will never be greater than 100, we can put a lower bound on the quantum yield for nonproton ions from the $\phi\Lambda$ data given in Table I. Dividing the $\phi\Lambda$ values by 100, it is clear that the quantum yield is usually >1 and in the case of the highest pH could be as high as 10. Note that any effect of light saturation would only reduce the apparent quantum yield—again, this is a lower bound estimate. (Some of the data in Table I were collected at higher light intensities for signal to noise reasons.) Thus there could still be protons being pumped at quantum yields similar to those observed by other workers (Govindjee et al., 1980; Ort and Parson, 1978) but the proton contribution would be small compared with the conductance changes due to the other ions. Given the substantial relative errors in the calculated ratios of the transient to the thermal signals (S_P/S_T), amplitude changes up to ~30% would be difficult to distinguish from noise. The one exception is at low pH (compare samples 1 *A* and 1 *H*) where there is a substantial population of free protons compared with buffering ions. Free hydrogen ion has an equivalent conductance 5 to 10 times larger than any of the charged buffer species, so even a small component of the total ion movement due to free protons would be proportionally more visible. As noted above, there was a

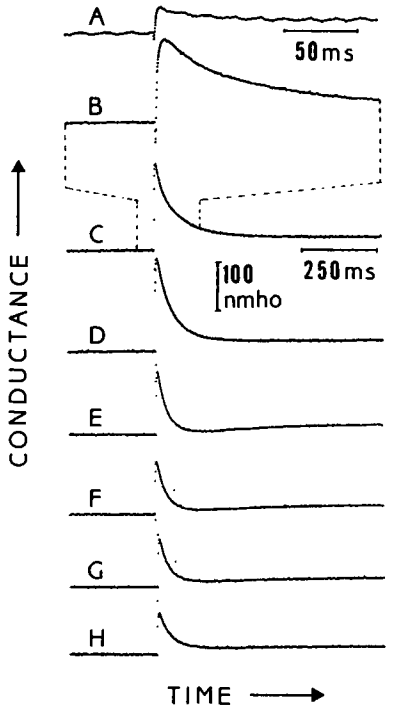

FIGURE 2 Effect of addition of Triton X-100 on light-induced conductivity changes in PM suspensions at pH 7 in 1.1 M NaCl. Solution conditions are in Table II, samples 5-*A*–5-*H*. Note that traces C–H are at five times longer sweep time; trace *C* is a repeat of *B*. Each trace is the sum of 64 flashes.

difference between unbuffered and acetate buffered solution at pH 5. If this difference was totally due to protons, it would correspond to a quantum yield of 0.46 ± 0.16 for the rapid proton uptake. The table also lists the decay time ($1/e$) of the conductance transient. As expected it is independent of the particular buffer at each pH. At low pH it is constant at 8 to 10 ms but increases at and above neutral pH.

The conductivity transients observed in PM suspensions at high ionic strength are primarily due to ions other than protons. To test if these ions are responding to changes in surface potential, we performed experiments in which the PM was either perturbed by addition of the nonionic detergent Triton X-100 or was completely solubilized in it.

Fig. 2 shows the effects of addition of Triton to PM fragments at pH 7. At low concentrations (0.024% vol/vol; traces *B* and *C*) the detergent causes a large increase in the signal amplitude—it corresponds to a quantum yield of 10 to 20 if due to sodium ions. Further increases up to 0.07% (trace *E*) cause the amplitude to decrease and the decay of the transient becomes distinctly biphasic: after a fast rise, the conductivity decreases below and then relaxes to the thermally shifted baseline. The "undershoot" is more pronounced at higher concentrations of detergent and lower pH; in some cases the signal goes below even the pre-flash baseline. Perturbation of the photocycle is evident from the 10-fold increase in the final decay time of the transient. However, as in the absence of Triton X-100, addition of phosphate in excess of imidazole buffer (traces *F*–*H*) does not change the sign of the signal.

TABLE II
bR WITH TRITON ADDED

#	pH	% TX	Imid	Phos	$\Sigma c_i\Lambda_i$	S_P	S_T	S_P/S_T	$\phi\Lambda$	% Err.	Relative signal	If H^+ only	Calculation of Λ per mole H^+	Decay time
														ms
5*A*	6.98	0	4.74	0	91.8	2.7	1.9	1.4	143	10	(1)	(1)	33.9	38
5*B*	6.98	0.024	4.72	0	91.8	12.9	1.7	7.6	777	10	5.4	1	33.9	51
5*C*	6.98	0.024	4.72	0	91.8	13.8	1.7	8.1	828	9	5.8	1	33.9	70
5*D*	6.95	0.047	4.69	0	91.8	15.6	1.4	11.1	1135	11	7.9	0.99	33.8	50
5*E*	6.93	0.070	4.67	0	93.3	9.7	1.8	5.4	561	8	3.8	0.99	33.8	30, 320
5*F*	7.00	0.070	4.64	4.64	93.3	7.7	1.8	4.3	447	8	3.1	−0.31	−10.5	30, 360
5*G*	7.05	0.069	4.60	9.21	95.7	7.0	1.7	4.1	437	9	3.1	−0.75	−25.5	32, 315
5*H*	7.18	0.068	4.50	22.5	91.8	6.0	1.7	3.6	368	10	2.6	−1.20	−40.7	40, 480
			GlyGly	GlyOEt										
6A	8.03	0	4.73	0	86.6	17.2	5.8	3.0	286	4	(1)	(1)	−24.3	100
6B	8.12	4.50	4.51	0	77.6	8.4	3.3	2.5	220	6	0.85	1	−24.4	1020
6C	8.00	4.49	4.49	4.49	77.6	4.9	3.4	1.4	124	7	0.49	−0.04	1.0	750
6D	8.08	4.45	4.45	8.91	74.3	5.3	3.0	1.8	146	8	0.59	−0.32	7.8	990
6E	8.06	4.39	4.39	17.6	75.6	4.2	2.8	1.5	126	9	0.51	−0.59	14.4	840
6F	8.08	4.29	4.29	34.3	75.6	3.3	2.7	1.2	103	9	0.41	−0.76	18.6	830

Effect of Triton addition on light induced conductance transients. bR in 1.1 M NaCl, pH 7 and 8. The Triton X-100 concentration (% vol/vol) is given in the "% TX" column. All other columns are as described in Table I.

Quantitation of these traces and a similar experiment at pH 8 is given in Table II. There is a decrease in $\phi\Lambda$ as the phosphate concentration is raised (samples 5 *F*–5 *H*) which could be due to protons, but it is at most 20% of the total signal. Increasing the detergent concentration over 50 times does not lead to the sign reversal upon buffer variation expected if protons alone were the cause of the transient. This is observed at pH 7 (not shown) and at pH 8 (Table II; samples 6 *A*–6 *F*). There is a decrease in amplitude, but this is ascribable equally well to a decrease in quantum yield in the presence of detergent (see below). The kinetic behavior is also affected: at pH 8 the decay time increases 10-fold; however, in alkaline solution we do not observe biphasic signals.

The experiments in which Triton X-100 is added to the sample are complicated by the slow solubilization of the PM, which is complete after 20 h at neutral pH (Dencher and Heyn, 1978). Also, we noted some chromophore loss at alkaline pH, which is reflected in the decrease of the thermal baseline. For that reason, we did not attempt to go to higher pH. Note that the presence of some bleached bR has no effect since it doesn't absorb at 590 nm and therefore does not contribute to the conductivity changes.

To separate the immediate effects of addition of Triton from the effect of complete solubilization, we prepared bR monomers in the detergent. The results are shown in Fig. 3 for two preparations solubilized in: (I) 0.33% vol/vol Triton, 25 mM potassium phosphate, pH 6.9 and (II) 0.38% vol/vol Triton, 5 mM imidazole, pH 6.7 respectively. The results are quite different from those of the previous experiments: in both cases, addition of the "opposing" buffer (phosphate is "acidic," imidazole is "basic") causes reversal of the sign of the transients as expected if the signal is due to fast proton release followed by slow uptake. These data were obtained using weak light flashes in the region of linear response, so that the ratio of the transient to the thermal signal would accurately reflect the quantum yield. This is responsible for the lower signal to noise in these traces. The quantitative analysis is presented in Table III. The buffer ion conductances used in these calculations were measured at 24°C at concentrations similar to those employed in the bR experiments, then corrected to 16°C. This is the most important correction, amounting to 20%. Other factors entering the calculation of the quantum yield such as the buffer *pK* values, solution heat capacity and the temperature coefficient of the mobility vary much less over this temperature range and their effect is neglected.

The result of the calculations is that the observed signals can be accounted for quite well, assuming that protons are the cause of the whole signal. The quantum yield calculated (0.07) is the same within experimental error in all cases. The value for sample I-C is higher than the others, although still reasonably close. This is in part due to the difficulty in estimating the equivalent conductance change for phosphate, which shows a strong dependence on concentration and on ionic strength. It may also reflect a dependence of the quantum yield on ionic strength since this sample contains considerably more total buffer salt than the others. But, the important observation is the reversal of the sign of the transient. The basic conclusion is that solubilization of the bR into monomers at pH 7 abolishes the nonproton ion movements seen with native PM fragments, which persist even immediately after addition of Triton X-100.

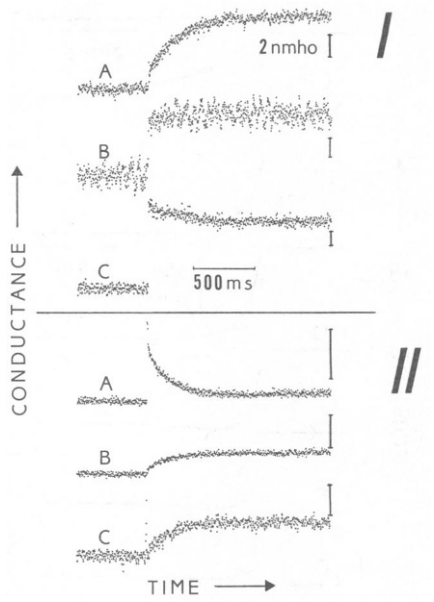

FIGURE 3 Light-induced conductivity changes in monomeric bR solubilized in Triton X-100 at pH 7. Note: absolute vertical scales are not the same between traces—the vertical bar at the end of each trace is 2 nmho. See Table III for data analysis. (*Part I*) bR in phosphate, then add imidazole. Pi, imidazole (in millimoles per liter) and pH are: *A*) 25, 0, 6.9; *B*) 24.3, 26, 6.88, and *C*) 22.9, 85.4, 6.92. Traces *A* and *C* are sum of 256 flashes; *B* is 128. (*Part II*) bR in imidazole, then add phosphate. Pi, imidazole (in mM) and pH are: *A*) 0, 5.07, 6.75; *B*) 6.2, 5.04, 6.72, and *C*) 12.3, 5.01, 6.70. All traces are sum of 128 flashes.

We also conducted experiments using bR solubilized in Triton in imidazole buffer at pH 7 then shifted to pH 4 with acetate or trimethylamine oxide. The results are given in Table IV. Qualitatively, the data behave as

TABLE III
bR SOLUBILIZED IN TRITON, pH 7

#	pH	Imid	Phos	$\Sigma c_i\Lambda_i$	S_P/S_T	$\phi\Lambda$	Λ_{eff}	ϕ_{H^+}	% error
I-A	6.90	0	25.0	3.48	−0.79	−2.93	−42	0.070	11
I-C	6.92	85.4	22.9	7.34	0.27	2.11	21	0.10	26
II-A	6.75	5.1	0	0.36	5.5	2.09	31	0.068	35
II-C	6.70	5.0	12.4	1.65	−0.93	−1.63	−25	0.065	32

bR solubilized in Triton X-100 at pH 7. Analysis of data of Fig. 3. Λ_{eff} is the effective equivalent conductance change for a proton (see Appendix) and ϕ_{H^+} is the quantum yield for transient proton release. Other terms are as in Table I.

TABLE IV
bR SOLUBILIZED IN TRITON, pH 4

#	pH	Imid	TMAO	OAc	S_P/S_T	$\phi\Lambda$	Λ_{eff}	ϕ_{H^+}	% error	Calculation of $\phi\Lambda$ if other ions than H^+
8A	4.02	5.00	4.96	0	−2.43	−2.91	57.6	−0.051	38	−2.87
8B	4.10	4.96	4.65	58.2	0.21	0.45	−24.5	−0.018	33	0.71
8C	3.99	4.94	0	9.89	0.48	0.39	−9.0	−0.043	47	0.03
8D	4.05	4.86	15.2	9.72	−0.48	−1.12	15.8	−0.071	31	−1.05

bR solubilized in Triton X-100 at pH 4. Terms as for Tables I and III. The last column is the calculated value of $\phi\Lambda$ assuming that it is the sum of contributions from protons (ϕ_{H^+} = 0.044) and "other ions" constant at $\phi\Lambda$ = 0.36. See text.

though at least part of the signal is due to protons (at this pH proton uptake precedes release): in both cases, the signal sign is negative with trimethylamine oxide as the dominant buffer and positive with acetate. However, the calculated quantum yields for proton release are not constant even considering the experimental error. Note that the yields are always higher in the amine oxide buffer than in acetate, i.e., when the observed transient is negative as opposed to positive. One plausible explanation is that there is a constant negative component in the transient that adds to the component due to protons. This would be due to the uptake of some other ion at the same time as proton uptake occurs. The results of a linear least-squares fit of the data are given in the last column of the Table. The calculated $\phi\Lambda$ values are based on a quantum yield for proton uptake of 0.044 and an "other ion" contribution to $\phi\Lambda$ of −0.36. If this were due to an ion like sodium, it would correspond to a quantum yield of 0.008.

DISCUSSION

The data presented in Fig. 1 and Table I show clearly that the conductivity changes observed in pulse-illuminated bR in 1.1 M NaCl are predominantly due to ions other than protons since the signals are unaffected by variation of the buffer at each pH. Our experience with native PM is that transient movements of protons alone occur only with the combination of low pH and low ionic strength.

Since our measurements are done with suspensions of PM fragments, we cannot distinguish ions that are transported across the membrane from those that are transiently released or taken up from the same side during the photocycle. If these ions were being pumped, one might expect some specificity. However, the nonproton ion movements shown above were also seen (with similar quantum yield) in our earlier reported experiments, performed at pH 8 in a buffer containing none of the ionic species present in this work. Thus the ion movements seem not to depend on the presence of a specific ion, e.g., Na^+.

A reasonable hypothesis is that the conductivity changes reflect alterations in the distribution of the PM's surface charges during the photocycle that result in counterions being released or taken up. This could result from a conformational change such as those inferred from circular dichroism (Gibson and Cassim, 1985) and photo-induced linear dichroism (Ahl and Cone, 1984). The latter authors suggest that when one bR molecule is excited, it induces similar chromophore rotations in its unexcited neighbors in the trimer. If these changes cause corresponding surface charge rearrangements the high observed quantum yields for ion movement could be more easily understood since one photon effectively "excites" three bR molecules.

If the conductance changes arise from the summation of the surface charges on neighboring bR molecules and lipids, then they should be affected by treatment with detergent, and that is what we observe. Fig. 2 and Table II show that addition of Triton X-100 causes a signal increase at low concentration, possibly due to loosening or breaking up large aggregates of PM fragments which otherwise occlude portions of the solution and hence reduce the detected free ion signal. Higher detergent concentration alters the kinetics and amplitude of the observed transients but the nonproton ion movements are not abolished. This implies that the local density of surface charges is still largely intact. Complete solubilization should eliminate most if not all of the surface charge effects since the charged molecules of the PM are diluted into the uncharged detergent micelles. The data of Tables III and IV show that this is borne out qualitatively at pH 4 and quantitatively at pH 7. It is possible that the deviations from a "proton-only" signal at pH 4 are due to the formation of small aggregates of bR in the micelle that could exhibit local surface charge effects. It is known that it is more difficult to solubilize the PM at low pH or at neutral pH with added salt (Dencher and Heyn, 1978); this implies increased stability of the aggregated structure under these conditions.

The central result of this work is that under conditions close to physiological (high ionic strength and pH near neutrality or somewhat alkaline), the bR photocycle causes large-scale ion movements that cannot be due to protons. At low pH this represents ion binding by the PM immediately after the flash; at netural pH and above the reverse is the case. It is to be emphasized strongly that these qualitative conclusions on the time sequence of the ion uptake or release are independent of any particular theory used to

describe the relation of the movement of the charges to the surface potential. The conductivity measurements are direct and absolute: ions that are trapped in the potential well at the membrane surface do not contribute—they effectively screen the PM fragment's charge and move with it. Our probe of surface potential changes is provided by the trapped counterions themselves. At neutral pH the depth of the electrostatic potential well must first decrease, and at low pH it must first increase, when bR goes through its photocycle.

This conclusion is at variance with some previous reports of light-induced surface charge changes in bR measured indirectly using charged probe molecules. Carmeli and Gutman (1982) used a pH-indicating dye, bromocresol green, in buffered solution and observed fast optical changes. These were interpreted as being caused by a shift in the *pK* of the bound indicator due to transient changes in the surface charge density of the PM. In the time frame relevant to our experiments, an increase in absorbance is observed that corresponds to an increase in the concentration of the deprotonated (charged) form of the dye and a more positive surface potential. We infer from their figures that the change is small—about 0.0002 absorbance units per flash relative to the post-flash baseline. There is an alternative explanation: using the *pK*s and concentrations of the buffer and dye used in these experiments, we calculate that ~0.1% of the protons taken up by the PM would come from the indicator. This would yield absorbance changes similar in sign and magnitude to those observed by Carmeli and Gutman. Hence, the absorbance changes in the time frame >1 ms are not necessarily due to a *pK* shift of the bound dye.

Other probe experiments used positively charged EPR spin labels (Carmeli et al., 1980; Tokutomi et al., 1980), in both cases a quaternary amine containing two methyl groups, a hydrophobic aliphatic chain, and the six-membered ring containing the paramagnetic center. Light-induced changes were observed in the relative amplitudes of the EPR signals associated with the "free" and the "bound" label that were interpreted as an increase in the negative surface potential of the PM. The first paper cited above reports that this potential change increases with pH by a factor of 2 from pH 2 to 10. Tokutomi et al. (1980) give data only for pH 5.8. While we do not disagree with the low pH results per se, there is a problem in that the concentration of the "probe" used is enormous—about seven spin labels per bR. Since the label is charged and has a hydrophobic tail, it can and does bind to the PM and thereby must alter the charge at the surface considerably. Castle and Hubbell (1976) validated the use of similar spin labels as probes of vesicle surface potential but were careful to work at label concentrations 100 times lower, both to avoid perturbing the surface charge of the vesicle by probe binding and to avoid paramagnetic broadening effects that can occur at high label concentrations. It would be interesting to see the behavior of the spin labels at lower concentration.

Light-induced potential changes have also been reported using a positively charged dye that exhibits shifts in its Raman spectrum associated with aggregation (Ehrenberg and Meiri, 1983; Ehrenberg and Berezin, 1984). Analysis of the Raman intensities indicates that at pH 6 the PM shows an increase in the negative charge density associated with the M412 intermediate. We also observe fast ion uptake followed by release at pH 6 so there is no conflict. Packer et al. (1984) measured the electrophoretic mobility of PM fragments and found that at pH 11 the mobility increases upon steady state illumination, indicating an increase in the surface charge density. They claim that they could not detect a change in charge at neutral pH. We do not have data at pH 11 and it is possible that the photocycle is too fast to give measurable steady state changes at the lower pH.

One obvious question that arises from our observation of large-scale nonproton ion movements is what kind of changes at the PM surface would be required to generate them. Most workers who have measured surface potential changes have interpreted their data in terms of the classical Gouy-Chapman theory (for reviews see McLaughlin, 1977 and Lee, 1977). This theory assumes that the surface charge can be approximated as being continously smeared over the surface of the membrane. At least qualitatively, it can account for the behavior of cations near negatively charged phospholipid bilayers (see for example, McLaughlin et al., 1971) although other workers have noted quantitative deviations due to discrete charge effects in both the binding of a fluorescent potential probe (Haynes, 1974) and in the electrochromic effect as a function of added salt in the thylakoid membrane (Tiemann and Witt, 1982).

The effect of localization of the charge is expected to be present in the case of the PM, where the charged amino acid side chains cannot diffuse and whose distribution is not expected to be homogeneous given the rigid structure of the purple membrane. Hence on a local scale modest movements of a few charged residues could have a great effect on the electrostatic potential within the bR even though the change in the average charge density is not very large. Also, one has to consider the ion condensation effect (Manning, 1978). When the distance of separation of discrete charges on a surface approaches a critical distance, of the order of the Coulomb radius in the particular solvent (in water ~7 Å at room temperature), the individual electrostatic potential wells centered on each charge overlap and a small mobile ion in the vicinity "sees" this longer range potential. Manning (1978 and references therein) has analyzed this effect for the case of an infinitely long cylindrical surface such as DNA. The essential features of the condensation are that the fraction of charges on the polyelectrolyte that are neutralized is primarily dependent only on the valence of the counterion and the

spacing of the discrete charges relative to the Coulomb radius. The fraction of bound counterions is independent of external salt over a broad range of concentration and does not go to zero in the limit of zero ionic strength. The ion condensation phenomenon has been extended to two-dimensional surfaces by Zimm and LeBret (1983). They find for an infinite homogenously charged plane, all of the counterions are condensed in the limit of infinite dilution no matter what the charge density is. Engstrom and Wennerstrom (1978) have solved the homogenous charge density problem for two parallel planes separated by an arbitrary distance and find that for the limit of infinite separation and reasonably high charge density the counterion distribution near the surface is independent of added salt.

The condensation of the ions is described by Manning as critical in the sense that a minimum critical charge density per unit length (for his one-dimensional polyelectrolytes) must be exceeded before the counterions condense. Our hypothesis as to the large-scale light-induced ion movements in the PM is that conformational changes in the protein cause changes in the distribution of the charges on the surface. For a discrete and heterogenous charge distribution as in the PM, there may be a critical "density" at which condensation occurs, unlike the predictions of idealized homogenous-distributed-charge models. The negatively charged lipids of the PM may adjust the overall charge density near the critical point. It is known that when bR is reconstituted in phospholipid vesicles it exhibits higher activity when the lipids are negative (Ramirez et al., 1981). We have some theoretical evidence (Raudino and Mauzerall, 1986) that a concave surface may accentuate the charge effects. Thus a conformational change of the protein could change the charge distribution or flatten or even invert a concave portion of the surface. Counterions would be released and then rebind when the bR returned to its original conformation. The time sequence of ion movement we observe correlates with that of proton movement: at low pH we see proton uptake before release and the ions follow suit; at neutral pH and above the release precedes uptake.

Given the large magnitude of the ion movements we observe, it is tempting to suggest that the changes in electrostatic potential that give rise to them are not simply passively following the photocycle but are part of the proton pump's driving force. It is known that the presence of charged groups on lipid membrane surfaces affects membrane conductivity (see Neumcke, 1970), even resulting in rectification if the charges are opposite. Several electrostatic models have been proposed for the proton pump in bacteriorhodopsin, in which the primary photochemical event results in a charge separation (see Birge et al., 1984 and references therein). While our conductivity method cannot directly measure charge movements in the protein itself, it is possible that the changes in the surface charge distribution that give rise to the ion movements we observe are manifestations of the primary electrostatic events, transmitted to the protein surface by a conformational change.

The closely packed arrangement of bR in the PM correlates nicely with an electrostatic model, since charge effects from close neighbors (e.g., members of the same trimer) would be additive. The contribution of an "electrostatic lever" to the operation of the pump is consistent with our observation that the quantum efficiency for proton release and uptake is lower in the monomeric bR than in the native PM. A similar process might be occurring in halorhodopsin, another retinal protein that acts as a chloride pump (Schobert and Lanyi, 1982). Conformationally driven surface potential changes would move any charge; the specificity could arise from a suitable selective filter, such as those found in the wide variety of ion-selective channels. (For a review of recent patch clamp studies, see Coronado and Labarca, 1984).

Our experiments do not probe the movement of charge through the PM—we only see the steps of the photocycle involving ion transfer to and from the aqueous phase. The next step is to determine whether the nonproton ion movements can be observed in oriented systems, i.e. where the two sides of the bR molecule can be spatially resolved. Such measurements are in progress.

APPENDIX

Effective Equivalent Conductance Change For Protons in Buffered Solutions

The basic problem is to calculate the distribution among the various buffering species upon addition of a small amount of strong acid. This problem has been covered for buffers of physiological interest in a recent book by Stewart (1981). Knowing the changes in the concentrations of each buffer ion, one calculates the effective proton equivalent conductance by taking the weighted average. As we shall show, particularly at neutral pH, even minute concentrations of buffers (e.g. carbon dioxide) cannot be neglected.

There are three species to consider: buffers that lose charge on protonation (e.g., acetate) or that gain charge (e.g., ammonia), hydroxide, and free hydrogen ion. Using the acid dissociation constant K_a of the buffer and the known total amount of buffer, one calculates the concentration of each of the buffer species as a function of the proton concentration. The condition of electrical neutrality gives a single polynomial in $[H^+]$:

$$\sum_i c_i Z_i = 0 = [H^+] - \frac{K_w}{[H^+]} + [M^+] - [X^-] + \sum_{\text{buffers}} \frac{(Z \cdot [H^+] + Z' \cdot K_a) \cdot B_0}{[H^+] + K_a}. \quad \text{(A1)}$$

Here $[M^+]$ and $[X^-]$ represent the concentrations of nonbuffering cations and anions, such as buffer counterions, added salt, etc. Z and Z' are the algebraic charge of the buffer ions in their acid and basic forms, respectively, and B_0 is the total concentration of each buffer present. This equation could be solved numerically. Using the calculated $[H^+]$, one

could then calculate the concentrations of each buffer ion. The effect of addition of strong acid is found by adding the appropriate amount to the $[X^-]$ term and resolving the equation.

If the changes are small, however, one can get an approximate solution in closed form by writing the charge conservation condition in differential form:

$$\sum_i Z_i \delta c_i = 0 = \sum_i Z_i \frac{\partial c_i}{\partial [H^+]} \cdot \delta[H^+] - \Delta c, \qquad (A2)$$

where Δc is the total amount of strong acid added. Explicit evaluation of the derivatives and signs gives

$$0 = \delta[H^+] \cdot \left\{1 + \frac{K_w}{[H^+]} + \sum_{\text{buffers}} \frac{B_0 K_a (Z - Z')}{([H^+] + K_a)^2}\right\} - \Delta c. \qquad (A3)$$

This is a simple linear equation in the change in the free proton concentration. Note that the terms in the summation are always positive since $Z-Z'$ is $+1$ for all types of buffers.

The magnitude of each of the terms is proportional to the fraction of added protons that at equilibrium will be free hydrogen ion, will have neutralized a hydroxyl ion or will have conbined with the buffers, respectively. The fraction of each species is simply its contribution divided by the whole sum.

Relatively low concentrations of buffer are needed to almost totally eliminate the contribution of free protons and free hydroxyl ions, especially near pH 7. Table V lists the size of the term due to H^+ plus OH^- at various pH values. Next to each is the concentration of a buffer with pK_a – pH, which will result in a term 100 times as large, i.e., which means 99% of the conductivity signal will be due to the buffer ions.

TABLE V

pH	$H^+ + OH^-$ term	Buffer conc for term 100 ×
		mM
4	1.00	40.0
5	1.00	4.0
6	1.02	0.41
7	2.00	0.08
8	101	0.4
9	10,000	4.0
10	1,000,000	40.0

Thus at pHs near neutrality, very low buffer concentrations are needed to very effectively buffer the solution. This is important in experiments such as those using pH-indicating dyes to measure proton release, since even small amounts of buffer can seriously influence the apparent proton yield. Also, small amounts of buffer, especially at neutral pH, could serve as a "reservoir" for protons. This could explain the observations of Drachev et al. (1984), who, in an elegant experiment, showed that the discrepancy between the kinetics of the rise of M412 and the release of protons could be eliminated by either increasing the concentration of the indicating dye (nitrophenol; pK 7.1) or by adding a small amount of MES buffer.

The effective equivalent conductance is obtained by multiplying the fractions by the change, including sign, in conductance between the protonated and deprotonated form of the buffer:

$$\Lambda = \frac{\Lambda_{H^+} + \Lambda_{OH^-} \cdot \frac{K_w}{[H^+]^2} + \sum_{\text{buffers}} (\Lambda_{\text{acid}} - \Lambda_{\text{base}}) B_0 K_a / ([H^+] + K_a)^2}{1 + K_w/[H^+]^2 + \sum_{\text{buffers}} B_0 K_a / ([H^+] + K_a)^2}. \qquad (A4)$$

This equation was used to calculate the values in the Tables in the text.

We thank Drs. A. Raudino and G. Manning for helpful discussions and I. Zielinksi-Large for technical assistance.

This work was supported by National Institutes of Health grant GM32955-01.

Received for publication 22 August 1985 and in final form 17 March 1986.

REFERENCES

Agard, D. A., and R. M. Stroud. 1982. Linking regions between helices in bacteriorhodopsin revealed. *Biophys. J.* 37:589–602.

Ahl, P. L., and R. A. Cone. 1984. Light activates rotations of bacteriorhodopsin in the purple membrane. *Biophys. J.* 45:1039–1049.

Birge, R. R., A. F. Lawrence, T. M. Cooper, C. T. Martin, D. F. Blair, and S. I. Chan. 1984. The energetics and molecular dynamics of the proton pumping photocycle in bacteriorhodopsin. *In* Nonlinear Electrodynamics in Biological Systems. W. R. Adey and A. F. Lawrence, editors. Plenum Publishing Corp., NY.

Bogomolni, R. A., W. Hubbell, and W. Stoeckenius. 1986. Cation binding changes during the bacteriorhodopsin photocycle. *Biophys. J.* 49(2, pt. 2):212*a*. (Abstr.)

Carmeli, C., A. T. Quintanilha, and L. Packer. 1980. Surface charge changes in purple membranes and the photoreaction cycle of bacteriorhodopsin. *Proc. Natl. Acad. Sci. USA.*77:4707–4711.

Carmeli, C., and M. Gutman. 1982. Rapid light-induced surface charge changes in bacteriorhodopsin. *FEBS (Fed. Eur. Biochem. Soc.) Lett.* 141:88–92.

Castle, J. D., and W. L. Hubbell. 1976. Estimation of membrane surface potential and charge density from the phase equilibrium of a paramagnetic amphiphile. *Biochemistry.* 15:4818–4831.

Coronado, R., and P. P. Labarca. 1984. Reconstitution of single ion-channel molecules. *Trends Neurosci.* 7:155–160.

Dean, J. A., editor. 1979. Lange's Handbook of Chemistry. 12th edition. McGraw-Hill, Inc., NY.

Dencher, N. A. 1983. The five retinal-protein pigments of halobacteria: bacteriorhodopsin, halorhodopsin, P565, P370 and slow-cycling rhodopsin. *Photochem. Photobiol.* 38:753–767.

Dencher, N. A., and M. P. Heyn. 1978. Formation and properties of bacteriorhodopsin monomers in the non-ionic detergents octyl-B-D-glucoside and Triton X-100. *FEBS (Fed. Eur. Biochem. Soc.) Lett.* 96:322–326.

Dencher, N. A., and M. P. Heyn. 1979. Bacteriorhodopsin monomers pump protons. *FEBS (Fed. Eur. Biochem. Soc.) Lett.* 108:307–310.

Dencher, N. A., and M. P. Heyn. 1982. Preparation and properties of monomeric bacteriorhodopsin. *Methods Enzymol.*88:5–10.

Dencher, N. A., and M. Wilms. 1975. Flash photometric experiments on the photochemical cycle of bacteriorhodopsin. *Biophys. Struct. Mech.* 1:259–271.

Drachev, L. A., A. D. Kaulen, and V. P. Skulachev. 1984. Correlation of photochemical cycle, H^+ release and uptake and electric events in bacteriorhodopsin. *FEBS (Fed. Eur. Biochem. Soc.) Lett.* 178:331–335.

Druckmann, S., and M. Ottolenghi. 1981. Electric dichroism in the purple membrane of *Halobacterium halobium. Biophys. J.* 33:263–268.

Ehrenberg, B., and Y. Berezin. 1984. Surface potential on purple membranes and its sidedness studied by a resonance Raman dye probe. *Biophys. J.* 45:663–670.

Ehrenberg, B., and Z. Meiri. 1983. The bleaching of purple membranes does not change their surface potential. *FEBS (Fed. Eur. Biochem. Soc.) Lett.* 164:63–66.

Engelman, D. M., R. Henderson, A. D. McLachlan, and B. A. Wallace. 1980. Path of the polypeptide in bacteriorhodopsin. *Proc. Natl. Acad. Sci. USA.*77:2023–2027.

Engstrom, S., and H. Wennerstrom. 1978. Ion condensation on planar surfaces. A solution of the Poisson-Boltzmann equation for two parallel charged plates. *J. Phys. Chem.* 82:2711–2714.

Fisher, K. A., K. Yanagimoto, and W. Stoeckenius. 1978. Oriented absorption of purple membrane to cationic surfaces. *J. Cell Biol.* 77:611–621.

Gibson, N. J., and J. Y. Cassim. 1985. Crosslinking of bacteriorhodopsin provides further support for the deformation wave model of proton transport. *Biophys. J.* 47 (2, pt. 2):94*a*. (Abstr.)

Govindjee, R., T. G. Ebrey, and A. R. Crofts. 1980. The quantum efficiency of proton pumping by the purple membrane of *Halobacterium halobium*. *Biophys. J.* 30:231–242.

Happe, M., R. M. Teather, P. Overath, A. Knobling, and D. Oeterhelt. 1977. Direction of proton translocation in proteoliposomes formed from purple membrane and acidic lipids depends on the pH during reconstitution. *Biochem. Biophys. Acta.* 465:415–420.

Haynes, D. H. 1974. 1-Anilino-8-Naphthalenesulfonate: a fluorescent indicator of ion binding and electrostatic potential on the membrane surface. *J. Membr. Biol.* 17:341–366.

Henderson, R. 1977. The purple membrane from Halobacterium halobium. *Annu. Rev. Biophys. Bioeng.* 6:87–109.

Jap, B. K., M. F. Maestre, S. B. Hayward, and R. M. Glaeser. 1983. Peptide-chain secondary structure of bacteriorhodopsin. *Biophys. J.* 43:81–89.

Keszthelyi, L. 1980. Orientation of membrane fragments by electric field. *Biochim. Biophys. Acta.* 598:429–436.

Kimura, Y., A. Ikegami, K. Ohno, S. Saigo, and Y. Takeuchi. 1981. Electric dichroism of purple membrane suspensions. *Photochem. Photobiol.* 33:435–439.

Kushwaha, S. C., M. Kates, and W. Stoeckenius. 1976. Comparison of purple membrane from *Halobacterium cutirubrum* and *Halobacterium halobium*. *Biochim. Biophys. Acta.* 426:703–710.

Lee, A. G. 1977. Lipid phase transition and phase diagrams. I. Lipid phase transitions. *Biochim. Biophys. Acta.* 472:237–281.

Lozier, R. H., W. Niederberger, R. A. Bogomolni, S.-B. Hwang, and W. Stoeckenius. 1976. Kinetics and stoichiometry of light-induced proton release and uptake from purple membrane fragments, *Halobacterium halobium* cell cenvelopes, and phospholipid vesicles containing oriented purple membrane. *Biochim. Biophys. Acta.* 440:545–556.

Manning, G. M. 1978. The molecular theory of polyelectrolyte solutions with applications to the electrostatic properties of polynucleotides. *Q. Rev. Biophys.* 11:179–246.

Marinetti, T., and D. Mauzerall. 1983. Absolute quantum yields and proof of proton and nonproton transient release and uptake in photoexcited bacteriorhodopsin. *Proc. Natl. Acad. Sci. USA.* 80:178–180.

Marinetti, T., and D. Mauzerall. 1985. Effect of Triton X-100 on light-induced ion release from purple membranes. *Biophys. J.* 47 (2, Pt. 2):96*a*. (Abstr.)

McLaughlin, S. 1977. Electrostatic potentials at membrane-solution interfaces. *Curr. Top. Membr. Trans.* 9:71–144.

McLaughlin, S. G. A., G. Szabo, and G. Eisenman. 1971. Divalent ions and the surface potential of charged phospholipid membranes. *J. Gen. Physiol.* 58:667–687.

Mitchell, D., and G. W. Rayfield. 1986. Order of proton uptake and release by bacteriorhodopsin at low pH. *Biophys. J.* 49:563–566.

Neugebauer, D. C., D. Oesterhelt, and H. P. Zingsheim. 1978. The two faces of the purple membrane. II. Differences in surface charge properties revealed by ferritin binding. *J. Mol. Biol.* 125:123–135.

Neumcke, B. 1970. Ion flux across lipid bilayer membranes with charged surfaces. *Biophysik.* 6:231–240.

Oesterhelt, D., and W. Stoeckenius. 1973. Functions of a new photoreceptor membrane. *Proc. Natl. Acad. Sci.* 70:2853–2857.

Oesterhelt, D., and W. Stoeckenius. 1974. Isolation of the cell membrane of *Halobacterium halobium* and its fractionation into red and purple membrane. *Methods Enzymol.* 31:667–678.

Ort, D. R., and W. W. Parson. 1978. Flash-induced volume changes of bacteriorhodopsin-containing membrane fragments and their relationship to proton movements and absorbance transients. *J. Biol. Chem.* 253:6158–6164.

Ovchinnikov, Y. A., N. G. Abdulaev, M. Y. Feigina, A. V. Kiselev, and N. A. Lobanov. 1979. The structural basis of the functioning of bacteriorhodopsin: an overview. *FEBS (Fed. Eur. Biochem. Soc.) Lett.* 100:219–224.

Packer, L., B. Arrio, G. Johannin, and P. Volfin. 1984. Surface charge of purple membranes measured by laser Doppler velocimetry. *Biochem. Biophys. Res. Commun.* 122:252–258.

Ramirez, F., H. Okazaki, and S.-I. Tu. 1981. Effect of phospholipid composition on activities of bacteriorhodopsin in reconstituted purple membranes. *FEBS (Fed. Eur. Biochem. Soc.) Lett.* 135:123–126.

Ramirez, F., H. Okazaki, S. Tu, and H. Hutchinson. 1983. Proton movements in reconstituted purple membrane of *Halobacteria:* effect of pH and ionic composition of the medium. *Arch. Biochem. Biophys.* 222:464–472.

Raudino, A., and D. C. Mauzerall. 1986. The effect of local geometry on ion binding to proteins. *Biophys. J.* 49(2, Pt. 2):492*a*. (Abstr.)

Renthal, R. 1981. Light-induced changes in H^+ binding to the purple membrane. *J. Biol. Chem.* 256:11471–11476.

Schobert, B., and J. K. Lanyi. 1982. Halorhodopsin is a light-driven chloride pump. *J. Biol. Chem.* 257:10306–10313.

Slifkin, M. A., H. Garty, and S. R. Caplan. 1978. Modulation-excitation methods in the study of bacteriorhodopsin. *In* Energetics and Structure of Halophilic Microorganisms. S. R. Caplan and M. Ginzburg, editors. Elsevier/North-Holland Biomedical Press. 165–184.

Slifkin, M. A., H. Garty, W. V. Sherman, M. F. P. Vincent, and S. R. Caplan. 1979. Light-induced conductivity changes in purple membrane suspensions. *Biophys. Struct. Mech.* 5:313–320.

Stewart, P. A. 1981. How to Understand Acid-Base. Elsevier, New York. 186 pp.

Stoeckenius, W., and R. A. Bogomolni. 1982. Bacteriorhodopsin and related pigments of *halobacteria*. *Annu. Rev. Biochem.* 52:587–616.

Stoeckenius, W., R. H. Lozier, and R. A. Bogomolni. 1979. Bacteriorhodopsin and the purple membrane of *halobacteria*. *Biochim. Biophys. Acta.* 505:215–278.

Tiemann, R., and H. T. Witt. 1982. Salt dependence of the electrical potential at the photosynthetic membrane in steady-state light and its structural consequence. *Biochim. Biophys. Acta.* 681:202–211.

Tokutomi, S., T. Iwasa, T. Yoshizawa, and S. Ohnishi. 1980. Flash-induced fast change on purple membrane surface detected by spin-label method. *FEBS (Fed. Eur. Biochem. Soc.) Lett.* 114:145–148.

Washburn, E. W., editor. 1929. International Critical Tables. Vol. VI, 1st edition. McGraw Hill, Inc. New York.

Zimm, B. H., and M. LeBret. 1983. Counter-ion condensation and system dimensionality. *J. Biomolec. Struct. Dynam.* 1:461–471.